Colloid Polym Sci (2014) 292:557–566
DOI 10.1007/s00396-013-3095-6

ORIGINAL CONTRIBUTION

# Dielectric relaxation behavior of ternary systems of water/toluene/Triton X-100: the effects of water and oil contents on microemulsion structure

**Kai Chen · Kongshuang Zhao**

Received: 28 June 2013 / Revised: 12 September 2013 / Accepted: 12 October 2013 / Published online: 31 October 2013


**Abstract** Dielectric relaxation studies were conducted on the ternary systems of the nonionic surfactant Triton X-100 (a nonionic surfactant with a polyoxyethylene chain)/toluene/water in the frequency range from 40 Hz to 110 MHz. The contents of water and toluene were varied separately while the ratios of the other two components were fixed. Remarkable dielectric relaxations were observed around 1 MHz and dielectric intensity shows different variation with the increase of the contents of water or toluene. Dielectric parameters were obtained by fitting the data using the Cole–Cole equation with one dispersion term. The reverse micelles, water-in-oil, and oil-in-water micro-regions of the microemulsions were identified by the dependence of conductivity of the dispersed phase and continuous phase on the contents of water or toluene. Hanai theory and the corresponding analysis method were used to calculate the phase parameters of the constituent phases. The analysis results suggest that the dielectric relaxation probably arises from the interfacial polarization.

**Keywords** Microemulsions · Dielectric analysis · Phase behavior · Interfacial polarization

## Introduction

Microemulsions are microheterogeneous, thermodynamically stable, spontaneously formed mixtures of oil and water under certain conditions by means of surfactants, with or without the aid of a cosurfactant [1]. Low interfacial tension and strong capacities of solubilization and emulsification are the basis of their applications [2]. The application field of microemulsions has been greatly broadened during the past decades. They can be utilized in oil recovery [3, 4], pollution control [5], nanoparticle fabrication [6, 7], industries for food [8, 9], pharmaceuticals [10], etc.

The phase behavior of microemulsions associated with the interfacial dynamics of the amphiphilic film, the mechanism of solubilization of the dispersed phase, and the reorganization of the microemulsions are difficult to clarify [11]. The temperature, the molecular structures of surfactant and cosurfactant, the type of oil, the water–oil ratio, and salinity could affect the phase behavior of the microemulsions [12]. For better insight into microemulsions, it is necessary to investigate their microstructures and structural transitions, which can be determined by various methods, such as conductivity [13, 14], electron microscopy [15–17], differential scanning calorimetry [18, 19], small angle X-ray scattering [20–22], fluorescence quenching [23, 24], nuclear magnetic resonance [16, 25, 26], etc. Although many studies have addressed the type and the structure of microemulsions, their physicochemical properties are still far from being well understood. More characterization methods are highly desired to be employed.

Dielectric relaxation spectroscopy (DRS), which measures permittivity and conductivity as a function of frequency in a noninvasive way, has been extensively in the characterization of all kinds of materials [27]. In recent years, DRS has become one of the most effective methods to detect the structural changes and electrical properties for microheterogeneous systems such as micellar solutions [28, 29] and microemulsions [30–35] at the molecular levels.

So far, there are only a few experimental studies on dielectric relaxation behavior of microemulsions. Some

K. Chen · K. Zhao (✉)
College of Chemistry, Beijing Normal University,
Beijing 100875, China
e-mail: zhaoks@bnu.edu.cn

studies emphasized the influence of temperature [30, 31], and others focused on the constituent dependence on dielectric relaxation behavior of microemulsions [32, 33]. For instance, the complex permittivity of microemulsion of water/isooctane/AOT (sodium bis(2-ethylhexyl)sulfosuccinate) has been studied by Ponton et al. [32], which shows that the electrical conductivity can be well described by a dynamic percolation model. The behavior of the relaxation frequency also agrees well with the scaling power laws of the dynamic percolation model. Tanaka et al. [33] have measured the permittivity and the electrical conductivity as a function of the molar ratio of water to AOT for the AOT microemulsion system with heptane, octane, and decane, respectively. The results showed that aggregation process strongly depends on the types of oil and the molar ratio. Asami [30] has used a spherical model to calculate the permittivity and conductivity of the constituent phases of Triton X-100/toluene/aqueous solution of 10 mM KCl systems. It has been found that dielectric relaxation markedly depends on the temperature from 20 to 40 °C, and the results were well interpreted in terms of interfacial polarization with a percolation model. Buchner et al. [31] have studied the influence of temperature on the water (W)/oil (O) microemulsions of water/*n*-octane/$C_{12}E_5$ by using the dilute salt solution as a "doted" model. The dielectric relaxation behavior is observed to be similar to the percolation of ionic W/O microemulsions. Recently, we have analyzed the dielectric relaxation behavior of APG/*n*-butanol/cyclohexane/water microemulsions with different water content [34]. In another work of ours [35], based on dc conductivity of [bmim][$PF_6$]/Triton X-100/water microemulsion systems, the static percolation process and the microcosmic picture showed multiple polarization mechanism on mesoscopic and microcosmic scale in a wide frequency range.

As mentioned above, a microemulsion is a dynamic system with adjustable properties, which allows a study of the influence of various parameters on microemulsion structure. Triton X-100 (polyethylene glycol *p*-(1,1,3,3-tetramethylbutyl)-phenyl ether) is a typical nonionic surfactant, with specific applications in cell biology and frequently used in industrial or household detergents. For example, reverse micelles can be formed with Triton X-100 in cyclohexane [36], toluene [37], and xylene [38]. It has been noted that the contents of water and oil have great effect on the microstructure of Triton X-100/toluene/water microemulsions [39]. In addition, the nonionic surfactant microemulsions can avoid the influence of electrode polarization on the dielectric behavior at low frequency [31]. Therefore, the ternary system of Triton X-100/toluene/water is particularly suitable for basic research by DRS.

In our study, we have investigated the effects of water amount (fixing the mass ratio of Triton X-100/toluene) and oil amount (fixing the mass ratio of Triton X-100/water) on the relaxation behavior of the microemulsions, which will be discussed in detail below. To facilitate DRS investigation, we replaced water by $10^{-3}$ mol $L^{-1}$ salt solution to provide sufficient charge carriers. It should be noticed that the addition of salt into water will not significantly affect the phase behavior of microemulsion. A relaxation which is considered as interfacial polarization can be observed in the frequency between 700 kHz and 25 MHz and will be analyzed and discussed by using Hanai equation. Based on these parameters, the effects of the contents of water and toluene on the relaxation behavior of the microemulsions are mainly focused. It is essential to explore the dynamics in these systems owing to their potential as microreactors [40].

## Experimental

### Preparation of microemulsions

Triton X-100 (polyethylene glycol *p*-(1,1,3,3-tetramethylbutyl)-phenyl ether) (A.R. grade) and toluene (A.R. grade) were purchased from Amresco Chemical Inc. (America) and Beijing Chemical Reagent Factory (China), respectively. Deionized water possessing a specific resistance higher than 16 MΩ $cm^{-1}$ was used as solvent, which was obtained from an AquaPro P Series water purification system (Taiwan, China). The structure of Triton X-100 is shown in Scheme 1. It was dried under vacuum at 80 °C for 12 h to remove excess water before use.

The microemulsions were prepared by mixing appropriate weight fractions of water, Triton X-100, and toluene. The experimental paths are shown in Fig. 1 in which the boundaries are drawn according to the work of Almgren et al. [37]; Path 1 illustrates the increase of water (4–28 wt%) when the weight ratio of toluene/Triton X-100 is fixed to 1:1. Path 2 illustrates the increase of toluene (6–54 wt%) when the weight ratio of water/Triton X-100 is fixed to 18:82.

### Dielectric measurements

The dielectric measurements were performed on a 4294A precision impedance analyzer from (Agilent Technologies) that allows a continuous frequency measurement from 40 Hz to 110 MHz. A dielectric measurement cell with concentrically cylindrical platinum electrodes was employed [41] and connected to the impedance analyzer by a 1607E spring clip fixture (Agilent Technologies). The cell constant

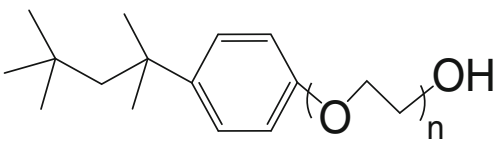


**Scheme 1** Chemical structure of Triton X-100. The average number of oxyethylene groups (*n*) is equal to 9.5

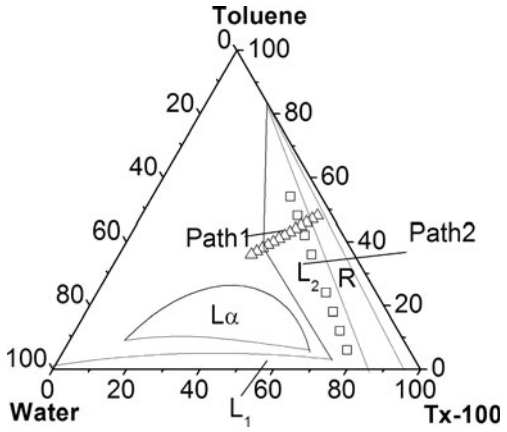


**Fig. 1** Experimental paths adopted in this work for Triton X-100/toluene/water systems: *triangle* (path 1) denotes the ternary systems when the weight ratio of Triton X-100/toluene is fixed as 1:1 with different water contents; *square* (path 2) shows the ternary systems which the weight ratio of Triton X-100/water is fixed as 82:18 with different toluene contents; the phase diagram at 24 °C is cited from reference [37]

and stray capacitance were determined with air, ethanol, and pure water. The measured dielectric data were corrected by the cell constant, stray capacitance, and residual inductance according to Schwan's method [42]. The permittivity and total dielectric loss at every measured frequency were calculated from the corrected capacitance and conductance.

### Determination of relaxation parameters

The parameters of dielectric relaxation, such as the limiting values of low and high frequency of permittivity and conductivity and the characteristic relaxation frequency, reflect the characteristics of DRS. These parameters can be obtained by fitting the Cole–Cole empirical equation [43] (Eq. (1)) to the experimental data:

$$\varepsilon^* = \varepsilon' - j\varepsilon'' = \varepsilon_h + \frac{\Delta\varepsilon}{1 + (j\omega\tau)^{\beta}} \quad (1)$$

where $\varepsilon^*$ is the complex permittivity, $\varepsilon'$ is the permittivity, $\varepsilon''$ is the dielectric loss, $\Delta\varepsilon(=\varepsilon_l - \varepsilon_h)$ is the relaxation intensity, $\varepsilon_l$ and $\varepsilon_h$ are the low- and high-frequency limits of relative permittivity, respectively, $\omega$ is the angular frequency ($\omega=2\pi f$, $f$ is the frequency), $\tau$ is the relaxation time, $\beta$ ($0<\beta\leq1$) is the Cole–Cole parameter indicating the dispersion of the relaxation time $\tau$, and $j^2=-1$. $\varepsilon''=(\kappa-\kappa_l)/\omega\varepsilon_0$, and $\tau=(2\pi f_0)^{-1}$ in which $\kappa$ is the conductivity, $\kappa_l$ is the low-frequency limit of conductivity, $\varepsilon_0$ is the permittivity of vacuum equal to $8.854\times10^{-12}$ F m$^{-1}$, and $f_0$ is the characteristic frequency.

## Results and discussion

### Effects of water content on the microemulsion structure

It is well known that water is one of the important components in microemulsions, and different water contents play a crucial role in the formation and structure of microemulsions. To investigate the effect of different water contents on the phase behavior of Triton X-100 reverse microemulsions, we choose experimental path 1 as described in Fig. 1.

Figure 2 shows the three-dimensional representations of the experimental results: Fig. 2a, b shows the frequency dependence of the permittivity and dielectric loss of ternary systems of Triton X-100/toluene/water with different water contents when the weight ratio of toluene/Triton X-100 is fixed as 1:1 (according to path 1 in Fig. 1). The directions of the increase of water mass concentration are shown by the arrows. An obvious dielectric relaxation can be seen from Fig. 2a, b. When the water contents $W_t(H_2O)\%\geq12$ %, a significant relaxation can be observed in the frequency of $10^5$–$10^6$, and the relaxation frequency changed little with the water content, but the relaxation intensity increased with the water contents. For clarity, the two-dimensional dielectric spectra of several water contents $W_t(H_2O)\%$ at 10,14, 18, and 22 % are shown in Fig. 3. Figure 3 also shows the best fitting results which are in good agreement with the

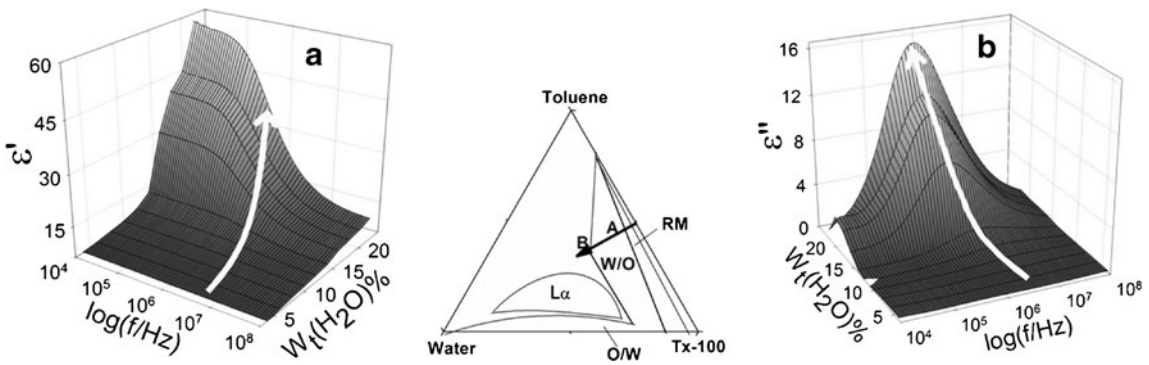


**Fig. 2** Three-dimensional representations for the frequency dependence of **a** permittivity and **b** dielectric loss of ternary systems of Triton X-100/toluene/water (when the weight ratio of toluene/Triton X-100 is fixed as 1:1) with different water contents. The directions of the increase of water mass concentration are shown by the *arrows*

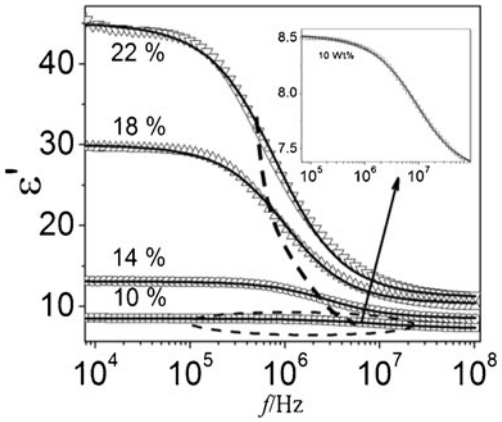


**Fig. 3** Relative permittivity spectra extracted from Fig. 2a at several water contents: (*square*) 10 %, (*circle*) 14 %, (*up-pointing triangle*) 18 %, and (*down-pointing triangle*) 22 %, respectively. The *symbols and the solid lines* represent the experimental data and the best fitting curves by Eq. (1), respectively

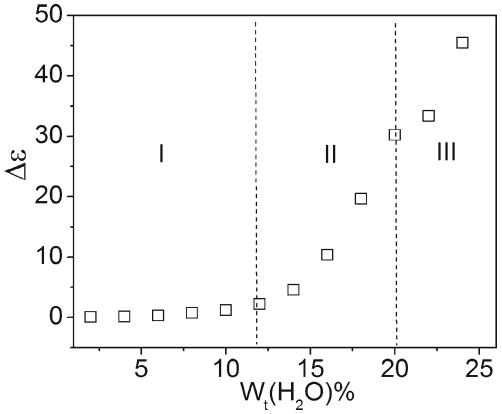


**Fig. 4** Dependence of $\Delta\varepsilon$ on the content of water when the weight ratio of toluene/Triton X-100 is fixed as 1:1; the *dotted lines* show the probable domains of different microstructures

experimental data. The dielectric parameters ($\varepsilon_l$, $\varepsilon_h$, $f_0$, and $\tau$) obtained by fitting experimental data with the Cole–Cole equation (Eq. (1)) are listed in Table 1.

The dielectric parameters of path 1

Figure 4 shows the dependence of dielectric intensity $\Delta\varepsilon$ on the content of water. $\Delta\varepsilon$ remains almost constant in reverse micelle (RM) region which is below point A in the phase diagram. This is probably because in the RM region the radius of the reverse micelles remains almost constant with the increase of water contents. In the W/O microemulsion region which is between points A and B in the phase diagram in Fig. 2, i.e., 13 %<$W_t(H_2O)$%<20 %, $\Delta\varepsilon$ sharply increases with the water contents (Fig. 4), indicating the increase of phase interface of the microemulsion droplets.

When $W_t(H_2O)$%>20 % (see the phase diagram in Fig. 2), the system enters into the multiple phase region, in which the W/O microemulsions are in equilibrium with excess water. With increasing water contents, $\Delta\varepsilon$ keeps a similar trend as in W/O region (Fig. 4), which indicated that W/O still occupied a major volume and kept the original huge phase interface in the multiple phase region. It shows that the change in microstructure of microemulsions can be well monitored by dielectric parameters.

**Table 1** Dielectric parameters of the microemulsion systems with different water contents when the weight ratio of toluene/Triton X-100 is fixed as 1:1

| $W_t(H_2O)$% | $\varepsilon_l$ | $\varepsilon_h$ | $\beta$ | $f_0$ (MHz) | $\tau$ (ns) | $\Delta\varepsilon$ | $\kappa_l$ ($10^6$×S/cm) |
|---|---|---|---|---|---|---|---|
| 4 | 5.95 | 5.78 | 0.79 | 23.1 | 6.88 | 0.17 | 0.41 |
| 6 | 6.68 | 6.36 | 0.76 | 17.7 | 8.98 | 0.32 | 0.59 |
| 8 | 7.63 | 6.90 | 0.74 | 13.6 | 11.70 | 0.73 | 0.83 |
| 10 | 8.52 | 7.29 | 0.75 | 8.99 | 17.70 | 1.23 | 0.85 |
| 12 | 10.02 | 7.80 | 0.78 | 4.99 | 31.90 | 2.22 | 0.96 |
| 14 | 13.13 | 8.53 | 0.82 | 2.86 | 55.7 | 4.60 | 1.30 |
| 16 | 19.61 | 9.26 | 0.83 | 1.50 | 106 | 10.31 | 1.84 |
| 18 | 30.00 | 10.31 | 0.82 | 0.99 | 162 | 19.69 | 4.05 |
| 20 | 40.85 | 10.63 | 0.80 | 0.79 | 200 | 30.22 | 8.10 |
| 22 | 45.15 | 11.10 | 0.79 | 0.76 | 209 | 34.05 | 13.1 |
| 24 | 58.55 | 12.10 | 0.78 | 0.73 | 217 | 46.45 | 17.9 |

The phase parameters of path 1

The phase parameters, such as the permittivity and conductivity of the continuous and dispersed phases and the volume fraction occupied by the dispersed phase, can reflect the internal properties. For the sake of simplicity in modeling the microstructures of W/O or O/W microemulsions, we suppose the spherical droplets dispersed in the continuous phase, and the Hanai theory [44, 45] and its relevant analytical method can be applied to the W/O and O/W microemulsions systems [30–35, 46–48]. This theory can be expressed as following:

$$\frac{\varepsilon^*-\varepsilon_i^*}{\varepsilon_a^*-\varepsilon_i^*}\left(\frac{\varepsilon_a^*}{\varepsilon^*}\right)^{1/3}=1-\Phi \tag{2}$$

where $\varepsilon_a{}^*(\varepsilon_a{}^*=\varepsilon_a-j\kappa_a/\omega\varepsilon_0)$ and $\varepsilon_i{}^*(\varepsilon_i{}^*=\varepsilon_i-j\kappa_i/\omega\varepsilon_0)$ are, respectively, the complex relative permittivities of the continuous and dispersed phase and $\Phi$ is the volume fraction of the dispersed phase.

From the characteristic frequency in the range of $10^5$–$10^7$ Hz as well as the microstructure of microemulsions, it is considered that the dielectric relaxation shown in Fig. 2 could be caused by the interfacial polarization. By using the Hanai equation and corresponding analytical method, the permittivity and conductivity of water droplets and oil phase (mixture of toluene and Triton X-100) in the microemulsions were calculated from the relaxation parameters in Table 1. The permittivity of continuous phase ($\varepsilon_a$) was obtained from the

**Table 2** Phase parameters of Triton X-100/toluene/water microemulsions with different water contents when the weight ratio of toluene/Triton X-100 is fixed as 1:1

| $W_t(H_2O)$% | $\kappa_a$ ($10^6$×S/cm) | $\varepsilon_i$ | $\kappa_i$ ($10^6$×S/cm) | $\Phi$ | $\tau_{MW}$/(ns) |
|---|---|---|---|---|---|
| 4 | 0.25 | 68.08 | 9.70 | 0.10 | 738.00 |
| 6 | 0.37 | 67.32 | 19.80 | 0.13 | 378.00 |
| 8 | 0.37 | 58.88 | 42.70 | 0.15 | 164.00 |
| 10 | 0.39 | 52.94 | 85.70 | 0.20 | 79.80 |
| 12 | 0.40 | 41.14 | 94.30 | 0.23 | 61.50 |
| 14 | 0.43 | 30.95 | 117.00 | 0.28 | 42.90 |
| 16 | 0.45 | 26.48 | 60.80 | 0.39 | 85.40 |
| 18 | 0.56 | 23.51 | 52.50 | 0.45 | 101.00 |
| 20 | 0.50 | 18.17 | 34.30 | 0.60 | 176.00 |
| 22 | 0.55 | 15.98 | 33.40 | 0.69 | 209.00 |
| 24 | 0.50 | 16.17 | 33.20 | 0.71 | 228.00 |

mixture of toluene and Triton X-100 in a weight ratio of 1:1, which was equal to 4.51 and was used as a known quantity. Table 2 shows the phase parameters determined in this analysis.

It can be seen from Fig. 5 that the water content is divided into three regions by the trend of the conductivity of the dispersed phase, and these three regions are the same as that shown in Fig. 4. This means that the phase parameters obtained by model calculation can denote the transition of the microstructure of microemulsions. Based on the changes of $\kappa_i$ in these three region, the dielectric relaxation behavior can be interpreted as follows: In the reverse micelle region ($W_t(H_2O)\% \leq 12$ %), $\kappa_i$ was enhanced with the increase of water, which shows that the diffusion and transport of internal conductive ions ($Na^+$ and $Cl^-$) in water droplets were accelerated; When $14 \leq W_t(H_2O)\% \leq 20$ %, $\kappa_i$ declines slightly because the combination between water molecules and the ethylene oxide (EO) units of Triton X-100 reaches saturation, and thus, a continuous addition of water could dilute the concentration of $Na^+$ and $Cl^-$ in internal phase. When $W_t(H_2O)\% > 20$ %, the content of water is increased but $\kappa_i$ keeps unchanged, probably because almost all of the increasing water enters into the lower aqueous phase. On the other hand, the values of the conductivity of the dispersed phase ($\kappa_i$) are much larger than that in the continuous phase ($\kappa_a$). The $\kappa_i$ value falls within the range of $9\times10^{-6}$~$1.2\times10^{-4}$ S/cm and fluctuates into three regions. In contrast, the continuous phase consists of a mixture of toluene and Triton X-100, and its conductivity value ($\kappa_a$) is in the range of $(2.5\sim5.6)\times10^{-7}$ S/cm and fluctuates little with the change of water content. It indicates that the water amount in the continuous phase could be neglected.

Figure 6 shows the dependence of permittivity of the dispersed droplets ($\varepsilon_i$) on the content of water. The values of $\varepsilon_i$ over all water content range are lower than that of pure water, i.e., 80. It is reasonable because in our model, the water droplets as dispersed phase include the head group of surfactant layer with low permittivity [49]. Moreover, $\varepsilon_i$ decreases linearly with the increase of water content in the microemulsions, which could be interpreted that the dipole moment of the bound water molecules by the hydrogen bond was reduced compared with that of water, resulting in the decrease of permittivity of the dispersed phase. Therefore, the decrease of permittivity is affected by the increase of water content until 20 %; When the water content exceeds 20 %, the system enters into multiple region in which W/O microemulsions and water coexist. Because the number of water droplets is almost constant, the value of $\varepsilon_i$ is stable in this region. It should be mentioned here that the model for calculating phase parameters by Hanai equation assumes that the oil phase consists of the surfactant hydrophobic chains and toluene as continuous medium, and the water droplet including the EO chains of Triton X-100 head group as dispersed phase. In addition, it should also be emphasized that, in multiple region, the value of $\varepsilon_i$ calculated just reflects the dispersed phase permittivity of W/O microemulsions,

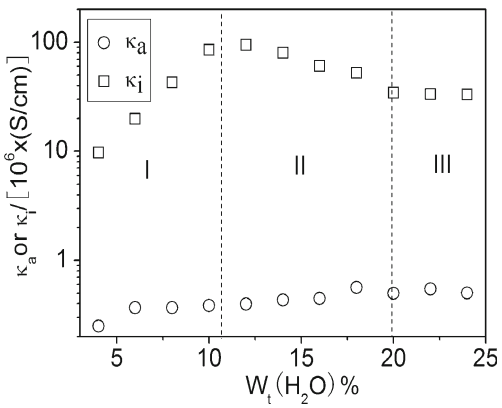


**Fig. 5** Dependence of $\kappa_a$ and $\kappa_i$ on the content of water when the weight ratio of toluene/Triton X-100 is fixed as 1:1. The *dotted lines* show the probable domains of different microstructures

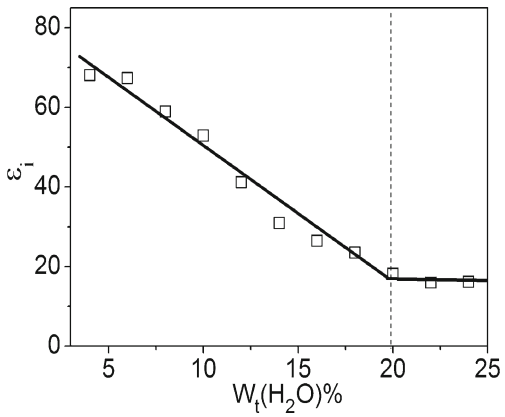


**Fig. 6** Dependencies of permittivity of the dispersed droplets $\varepsilon_i$ on the content of water

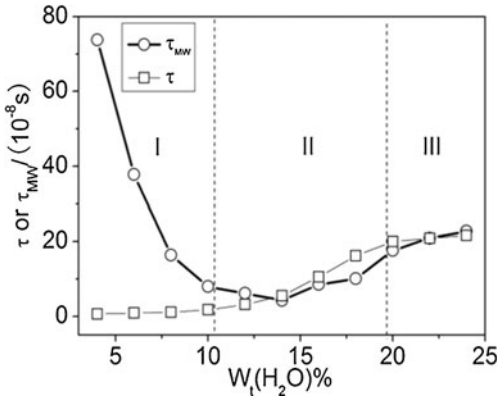


**Fig. 7** Dependence of $\tau_{MW}$ and $\tau$ on the water content when the weight ratio of toluene/Triton X-100 is fixed as 1:1

therein, and the volume fraction $\Phi$ refers to the percentage of spherical dispersed phase in W/O, which leads to a less adaptability for the Hanai model [34].

Relaxation mechanism of path 1

To determine the mechanism of the dielectric relaxation observed in this work, Eq. (3) was used to calculate the theoretical values of relaxation time ($\tau_{MW}$) from the phase parameters [49]. The results for the systems with different water contents are also listed in Table 2.

$$\tau_{MW} = \frac{2\varepsilon_i + \varepsilon_a + \phi(\varepsilon_i - \varepsilon_a)}{2\kappa_i + \kappa_a + \phi(\kappa_i - \kappa_a)}\varepsilon_0 \quad (3)$$

Figure 7 shows the dependence of theoretical relaxation time based on Maxwell–Wagner theory ($\tau_{MW}$) and the relaxation time observed experimentally ($\tau$) on the water content. It can be seen from Fig. 7 that when the water content is less than 10 %, the values of $\tau_{MW}$ and $\tau$ are quite different. With the increase of water content, $\tau_{MW}$ decreases sharply while $\tau$ keeps substantially constant, which cause the gap between $\tau_{MW}$ and $\tau$ gradually reduced. This verifies the mechanism of relaxation we mentioned above: The relaxation observed experimentally is indeed caused by the oil–water interfacial polarization. According to the differences between $\tau_{MW}$ and $\tau$ in the region of $W_t(H_2O)\%<10$ %, it at least implies that there is large error when we dealt with the reverse micelles using Hanai model because the layer of surfactant molecules was ignored in the model and this neglect is not appropriate. When $W_t(H_2O)\%>10$ %, in the region of reverse microemulsion, $\tau$ and $\tau_{MW}$ are consistent well with each other because the water droplets become larger and thus this neglect is reasonable thereafter.

Effects of toluene content on the microemulsion structure

Toluene and related compounds are important industrial solvents, and their decontamination from waste streams has been suggested via microemulsion routes. Toluene is aromatic and therefore expected to strongly interact with the central phenyl moiety of Triton X-100. When toluene was incorporated into a micelle, the micelle is expected to swell into dispersed droplets of oil. To investigate the effects of different toluene contents on the dielectric relaxation behavior of microemulsions, we choose experimental path 2 as described in Fig. 1.

Figure 8 shows the three-dimensional representations for the effects of toluene concentration on the dielectric spectra when the weight ratio of Triton X-100/water is fixed as 82:18 (according to the experimental path 2 shown in Fig. 1). It is obvious that Fig. 8 shows a dielectric relaxation process that is different from Fig. 2. In Fig. 8a, the relaxation intensity decreases with the increase of toluene content and the characteristic frequency can be confirmed in the range of $10^5$–$10^7$ by the position of the dielectric loss peak. In order to investigate the change of relaxation with increasing toluene contents in detail, the permittivity spectra in Fig. 8 for four toluene contents ($W_t(PhMe)\%=12$, 24, 36, and 48 %) are shown in Fig. 9. Figure 9 also shows the best-fit results, and the dielectric parameters obtained by fitting the experimental data with the Cole–Cole equation (Eq. (1)) are listed in Table 3.

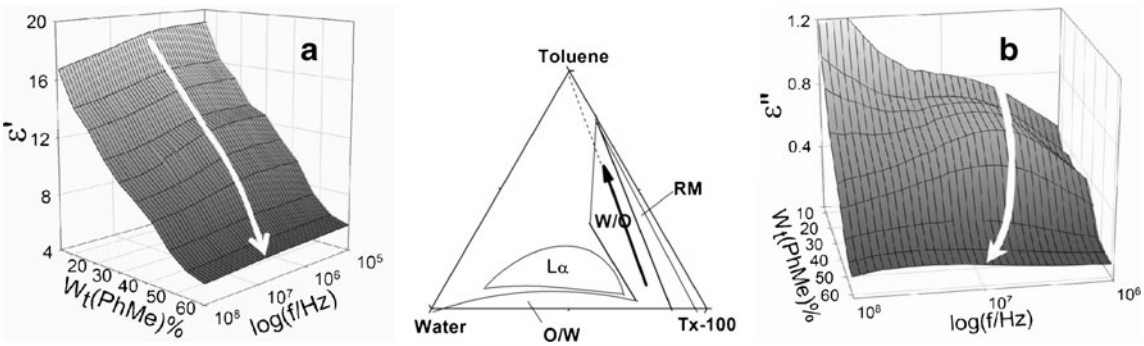


**Fig. 8** Three-dimensional representations for the frequency dependence of **a** permittivity and **b** dielectric loss of ternary systems of Triton X-100/toluene/water (when the weight ratio of Triton X-100/water is fixed as 82:18) on different toluene contents. The direction of the increase of toluene mass concentration is shown by *arrows*

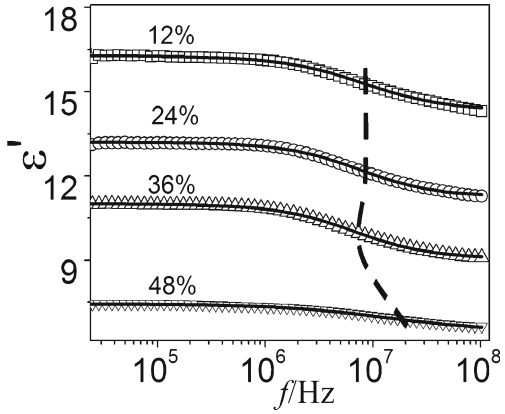


**Fig. 9** Experimental data and fitting curves of the dielectric relaxation at different toluene contents: (*square*) 12 %, (*circle*) 24 %, (*up-pointing triangle*) 36 %, and (*down-pointing triangle*) 48 % by the Cole–Cole equation. The weight ratio of Triton X-100/water is fixed as 82:18. The *symbols and the solid lines* represent the experimental data and the best fitting curves by Eq. (1), respectively

## Dielectric relaxation behaviors of path 2

Figure 10 shows the dependence of dielectric increment $\Delta\varepsilon$ on the content of toluene. It is worth noting that the value of $\Delta\varepsilon$ is divided into two regions at $W_t$(PhMe)%≈36 %: when $W_t$(PhMe)%≤36 %, $\Delta\varepsilon$ decreases with the increase of toluene content slowly, this phenomenon can be interpreted as the toluene molecules enter into the micelle cores resulting in the formation of O/W microemulsions, which result in the polarity of microemulsions to reduce. As the content of toluene increases to 36 %, the solubilization of toluene almost reaches saturation. After that, dielectric increment drastically reduced because the content of toluene in dispersed phase droplets increases rapidly. The continuous phase is transformed from the mixture of water/surfactant to the mixture of toluene/surfactant, while the core of the dispersed phase turns from toluene to water.

**Table 3** Dielectric parameters of the microemulsion systems with different toluene contents when the weight ratio of Triton X-100/water is fixed as 82:18

| $W_t$(PhMe)% | $\varepsilon_l$ | $\varepsilon_h$ | $\beta$ | $f_0$ (MHz) | $\tau$ (ns) | $\Delta\varepsilon$ | $\kappa_l$ ($10^6$×S/cm) |
|---|---|---|---|---|---|---|---|
| 6 | 19.12 | 16.81 | 0.72 | 8.62 | 18.47 | 2.31 | 15.10 |
| 12 | 16.31 | 14.28 | 0.74 | 8.18 | 19.45 | 1.82 | 12.90 |
| 18 | 15.03 | 13.04 | 0.79 | 7.25 | 21.95 | 1.99 | 10.70 |
| 24 | 13.21 | 11.23 | 0.84 | 6.84 | 23.26 | 1.98 | 7.33 |
| 30 | 12.58 | 10.74 | 0.85 | 6.27 | 25.40 | 1.89 | 5.79 |
| 36 | 11.00 | 9.20 | 0.85 | 5.62 | 28.31 | 1.80 | 3.03 |
| 42 | 9.62 | 8.04 | 0.79 | 7.59 | 20.97 | 1.54 | 1.48 |
| 48 | 7.45 | 6.54 | 0.73 | 12.75 | 12.48 | 0.89 | 0.49 |
| 54 | 6.19 | 5.46 | 0.68 | 21.42 | 7.43 | 0.57 | 0.24 |
| 60 | 5.68 | 5.21 | 0.72 | 22.87 | 6.96 | 0.47 | 0.20 |

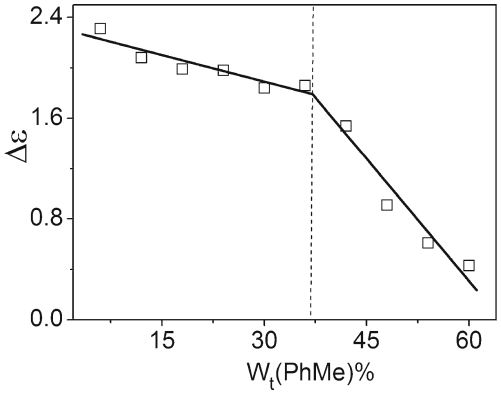


**Fig. 10** Dependence of $\Delta\varepsilon$ on the content of toluene when the weight ratio of Triton X-100/water is fixed as 82:18

Figure 11 shows the dependence of low-frequency limit of the conductivity ($\kappa_l$) on the content of toluene. Two regions are also observed in Fig. 11. It is found that the position of the break point is similar to that of $\Delta\varepsilon$ vs $W_t$(PhMe)% (Fig. 10). When $W_t$(PhMe)%≤36 %, with the increase of toluene, the content of water is reduced, which induces the conductivity to be reduced. When the content of toluene $W_t$(PhMe)% reaches 40 %, the solubilization of toluene almost reaches saturation. If we continue to increase the content of toluene, it will not obviously affect the conductivity. The results support that the continuous phase is transformed from the mixture of water/surfactant to the mixture of toluene/surfactant when the content of toluene is in the vicinity of 36 %. It shows that the variation of conductivity of the continuous phase with the contents of toluene can be well monitored.

## Phase parameters of path 2

The relaxation behavior of the microemulsions in the path 2 (shown in Fig. 1) can be characterized by relaxation increment and relaxation time. From the characteristic frequency in the

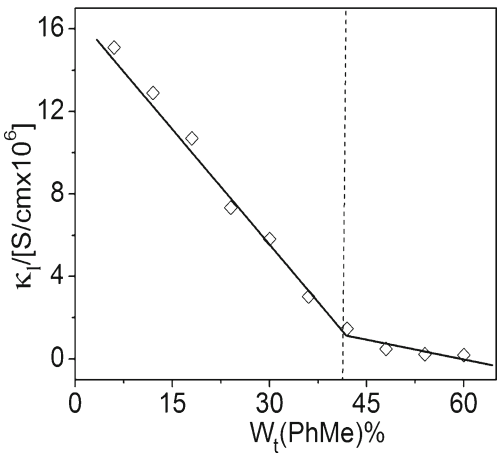


**Fig. 11** Dependence of $\kappa_l$ on the content of toluene when the weight ratio of Triton X-100/water is fixed as 82:18. The break point is denoted by the *dotted line*

**Table 4** Electrical phase parameters ($\Phi$, $\kappa_a$, $\varepsilon_i$, and $\kappa_{i)}$ with different toluene contents when the weight ratio of Triton X-100/water is fixed as 82:18

| $W_t$(PhMe)% | $\kappa_a$ ($10^6$×S/cm) | $\varepsilon_i$ | $\kappa_i$ ($10^6$×S/cm) | $\Phi$ | $\tau_{MW}$ (ns) |
|---|---|---|---|---|---|
| 6 | 13.97 | 2.44 | 2.04 | 0.197 | 36.41 |
| 12 | 12.88 | 2.46 | 1.29 | 0.294 | 48.32 |
| 18 | 10.74 | 2.44 | 1.06 | 0.355 | 55.24 |
| 24 | 7.56 | 2.42 | 0.70 | 0.434 | 76.00 |
| 30 | 6.11 | 2.43 | 0.54 | 0.463 | 94.65 |
| 36 | 1.47 | 2.46 | 0.28 | 0.539 | 185.73 |
| 42 | 0.767 | 56.51 | 42.63 | 0.198 | 12.11 |
| 48 | 0.304 | 47.31 | 16.62 | 0.146 | 26.17 |
| 54 | 0.166 | 40.51 | 4.00 | 0.116 | 93.16 |
| 60 | 0.139 | 35.56 | 2.99 | 0.093 | 296.17 |

range of $10^5$–$10^7$ Hz as well as the structure of microemulsions, we consider that the dielectric relaxation shown in Fig. 8 can be caused by the interfacial polarization.

By using Hanai equation and corresponding analytical method [44], the permittivity and conductivity of continuous and dispersed phases in the microemulsions were calculated from the relaxation parameters $\varepsilon_l$, $\varepsilon_h$, $\kappa_l$, and $\kappa_h$ in Table 3. The value of permittivity of continuous phase ($\varepsilon_a$) was obtained from the mixtures of Triton X-100/water or Triton X-100/toluene with various weight ratios, which is used as known quantity in computing. Table 4 shows the phase parameters determined in this analysis.

Figure 12 shows the dependence of conductivities of the continuous phase ($\kappa_a$) and dispersed phase ($\kappa_i$) on the content of toluene. It can be divided into two regions at the content of toluene being approximately 36 %. When $W_t$(PhMe)%≤36 %, the conductivity of the continuous phase ($\kappa_a$) gradually decreases with the increase of the toluene content, probably because the composition of the continuous phase is gradually transformed from the mixtures of Triton X-100/water to Triton X-100/toluene. Meanwhile, the conductivity of the disperse phase ($\kappa_i$) has remained fairly constant. When $W_t$(PhMe)% is near 36 %, the solubilization of toluene reaches saturation and the continuous phase almost completely consists of surfactants and toluene. Therefore, $\kappa_a$ is nearly constant thereafter. However, the conductivity of dispersed phase ($\kappa_i$) abruptly increases when $W_t$(PhMe)% reaches 36 % because the dispersed phase turns from toluene to water. Then, the $\kappa_i$ rapidly diminishes to the initial level because the core of water molecules changes from the free water to bound water.

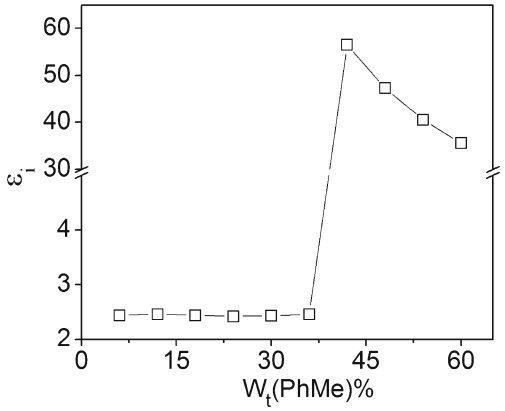


**Fig. 13** Dependence of permittivity of the dispersed phase ($\varepsilon_i$) on the content of toluene when the weight ratio of Triton X-100/water is fixed as 82:18

It is very meaningful that the permittivity changes with the content of toluene $W_t$(PhMe)%, especially the permittivity of the dispersed. Figure 13 shows the permittivity of dispersed phase is divided into two completely different regions in the vicinity of 36 % of the toluene content. When $W_t$(PhMe)%≤36 %, the value of $\varepsilon_i$ is approximately 2.4, indicating that the dispersed phase is organic phase; When the content of toluene exceeds 36 %, $\varepsilon_i$ abruptly increases to approximately 60, which means that the microemulsion has undergone a phase transition, implying that the composition of the dispersed phase changes from toluene to water. Then, $\varepsilon_i$ decreases from 60 to

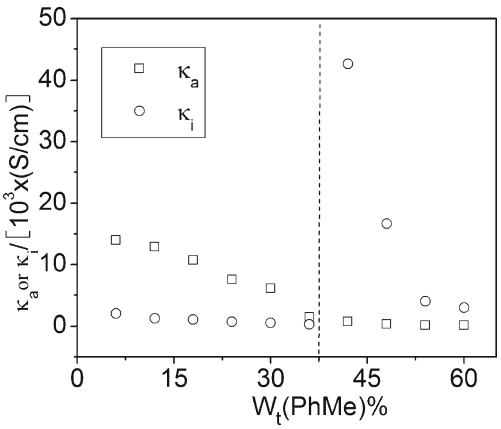


**Fig. 12** Dependence of $\kappa_a$ and $\kappa_i$ on the content of toluene when the weight ratio of Triton X-100/water is fixed as 82:18. The break point is denoted by the *dotted line*

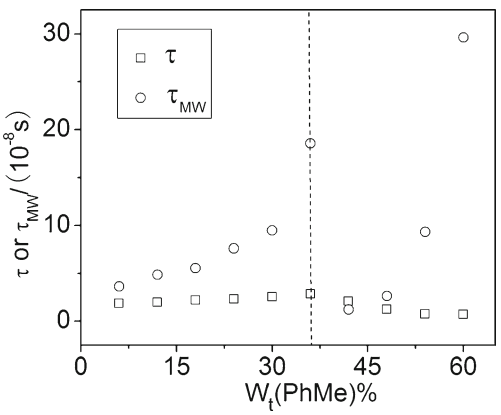


**Fig. 14** Dependence of $\tau_{MW}$ and $\tau$ on the content of toluene when the weight ratio of Triton X-100/water is fixed as 82:18

approximately 35, possibly because the core of water molecules changes from the free water to bound water.

Relaxation mechanism of path 2

For the discussion of the effects of toluene content, the theoretical relaxation time based on Maxwell–Wagner theory ($\tau_{MW}$) was also calculated by using Eq. (3), and the results are compared with the relaxation time experimentally ($\tau$) obtained by DRS from Table 3.

Figure 14 shows the dependence of $\tau_{MW}$ and $\tau$ on the toluene content. The values of $\tau_{MW}$ and $\tau$ are in the same order of magnitude when the content of toluene is below 36 %. Maxwell–Wagner theory can be used to explain the phenomenon because the system measured basically belongs to a typical dispersion system. When 36 %≤$W_t$(PhMe)%≤40 %, the values of $\tau_{MW}$ and $\tau$ are quite different because the phase interface is not obvious between the phase transition change from O/W to W/O. When 40 %≤$W_t$(PhMe)%≤50 %, $\tau_{MW}$ and $\tau$ get close again, the phase region accesses the W/O microemulsion which belongs to a typical dispersion system. It should be noted that it is relatively difficult to calculate relaxation time because phase interface becomes unapparent when $W_t$(PhMe)%>50 %.

## Conclusion

In this work, our main motivation is to investigate the dielectric relaxation behavior of ternary systems of Triton X-100/toluene/water in a wide frequency range. We have chosen two different experimental paths in order to get a meaningful overall picture for microemulsions. Striking dielectric relaxations were observed under the experiment conditions.

Through analysis of the relaxation time and relaxation increment dependence with the variation of water or toluene content, the break points in the plots of these parameters are consistent with the phase boundaries in the phase diagram. For turning point at 10 and 20 % in the path of water content while at 36 % in the path of toluene content changes, both the dielectric parameters and phase parameters imply the change of internal microstructure of the microemulsions. It showed that the dielectric relaxations occurred in different microstructure of microemulsions. Additionally, a direct measurement of phase behavior such as the conductivity is possible.

It proved that DRS is an effective method for detecting the microstructural characteristics of this microemulsion system. The dynamic information and the structural properties obtained by DRS will provide the theoretical foundation for other related studies.

**Acknowledgments** The financial support from the National Natural Scientific Foundation of China (nos. 21173025 and 20976015) and the Major Research Plan of NSFC (no. 21233003) is gratefully acknowledged.

## References

1. Danielsson I, Lindman B (1981) The definition of microemulsion. Colloids Surf 3(4):391
2. Fanun M (2010) Microemulsions: properties and applications, vol 144. CRC, New York, p 19
3. Nazar M, Shah S, Khosa M (2011) Microemulsions in enhanced oil recovery: a review. J Pet Sci Technol 29(13):1353
4. Hirasaki G, Miller C, Puerto M (2011) Recent advances in surfactant EOR. SPE J 16(4):889
5. Liu L, Tian S, Ning P (2010) Phase behavior of TXs/toluene/water microemulsion systems for solubilization absorption of toluene. J Environ Sci 22(2):271
6. Aubery C, Solans C, Sanchez-Dominguez M (2011) Tuning high aqueous phase uptake in nonionic water-in-oil microemulsions for the synthesis of Mn–Zn ferrite nanoparticles: phase behavior, characterization, and nanoparticle synthesis. Langmuir 27(23):14005
7. Kuang D, Xu A, Fang Y, Ou H, Liu H (2002) Preparation of inorganic salts ($CaCO_3$, $BaCO_3$, $CaSO_4$) nanowires in the Triton X-100/cyclohexane/water reverse micelles. J Cryst Growth 244(3):379
8. Spernath A, Aserin A (2006) Microemulsions as carriers for drugs and nutraceuticals. Adv Colloid Interface Sci 128:47
9. Deutch-Kolevzon R, Aserin A, Garti N (2011) Synergistic cosolubilization of omega-3 fatty acid esters and $CoQ_{10}$ in dilutable microemulsions. Chem Phys Lipids 164(7):654
10. Kljajic A, Bester–Rogac M, Klobcar A, Zupet R, Pejovnik S (2013) Crystallization using reverse micelles and water-in-oil microemulsion systems: the highly selective tool for the purification of organic compounds from complex mixtures. J Pharm Sci 102(2):330
11. Stubenrauch C (2009) Microemulsions: background, new concepts, applications, perspectives. Wiley, New York, p 25
12. Shah DO (1985) Macro- and microemulsions: theory and applications: based on a symposium, vol 272. American Chemical Society, New York, p 63
13. Bumajdad A, Eastoe J (2004) Conductivity of water-in-oil microemulsions stabilized by mixed surfactants. J Colloid Interface Sci 274(1):268
14. Li N, Ya G, Zheng L, Zhang J, Yu L, Li X (2007) Studies on the micropolarities of bmimBF4/TX-100/toluene ionic liquid microemulsions and their behaviors characterized by UV-visible spectroscopy. Langmuir 23(3):1091
15. Maxit B, Giermanska J, Ly I, Bendejacq D, Mondain-Monval O, Ponsinet V (2010) Freeze-fracture TEM imaging of robust order in swollen phases of amphiphilic diblock copolymers. Langmuir 27(5): 1990
16. Fanun M (2010) Formulation and characterization of microemulsions based on mixed nonionic surfactants and peppermint oil. J Colloid Interface Sci 343(2):496
17. Rai R, Baker GA, Behera K, Mohanty P, Kurur ND, Pandey S (2010) Ionic liquid-induced unprecedented size enhancement of aggregates within aqueous sodium dodecylbenzene sulfonate. Langmuir 26(23): 17821
18. Tzika ED, Christoforou M, Pispas S, Zervou M, Papadimitriou V, Sotiroudis TG, Leontidis E, Xenakis A (2011) Influence of nanoreactor environment and substrate location on the activity of horseradish peroxidase in olive oil based water-in-oil microemulsions. Langmuir 27(6):2692
19. Wu J, Yan H, Zhang X, Wei L, Liu X, Xu B (2008) Magnesium hydroxide nanoparticles synthesized in water-in-oil microemulsions. J Colloid Interface Sci 324(1):167
20. Tomšič M, Bešter-Rogač M, Jamnik A, Kunz W, Touraud D, Bergmann A, Glatter O (2004) Nonionic surfactant Brij 35 in water and in various simple alcohols: structural investigations by small-angle X-ray scattering and dynamic light scattering. J Phys Chem B 108(22):7021

21. Tabor RF, Zaveer MI, Dagastine RR, Grillo I, Garvey CJ (2013) Phase behaviour, small-angle neutron scattering and rheology of ternary nonionic surfactant-oil–water systems: a comparison of oils. Langmuir 29(11):3575
22. Naumann P, Becker N, Datta S, Sottmann T, Wiegand S (2013) Soret coefficient in nonionic microemulsions: concentration and structure dependence. J Phys Chem B 117(18):5614
23. Dong B, Zhao X, Zheng L, Zhang J, Li N, Inoue T (2008) Aggregation behavior of long-chain imidazolium ionic liquids in aqueous solution: micellization and characterization of micelle microenvironment. Colloids Surf A 317(1):666
24. Zana R, Schmidt J, Talmon Y (2005) Tetrabutylammonium alkyl carboxylate surfactants in aqueous solution: self-association behavior, solution nanostructure, and comparison with tetrabutylammonium alkyl sulfate surfactants. Langmuir 21(25):11628
25. Law SJ, Britton MM (2012) Sizing of reverse micelles in microemulsions using NMR measurements of diffusion. Langmuir 28(32):11699
26. Rao VG, Mandal S, Ghosh S, Banerjee C, Sarkar N (2013) Phase boundaries, structural characteristics, and NMR spectra of ionic liquid-in-oil microemulsions containing double chain surface active ionic liquid: a comparative study. J Phys Chem B 117(5):1480
27. Kremer F, Schönhals A (2003) Broadband dielectric spectroscopy. Springer, Berlin
28. Baar C, Buchner R, Kunz W (2001) Dielectric relaxation of cationic surfactants in aqueous solution. 1. Solvent relaxation. J Phys Chem B 105(15):2906
29. Baar C, Buchner R, Kunz W (2001) Dielectric relaxation of cationic surfactants in aqueous solution. 2. Solute relaxation. J Phys Chem B 105(15):2914
30. Asami K (2005) Dielectric relaxation in a water–oil-Triton X-100 microemulsion near phase inversion. Langmuir 21(20):9032
31. Schrödle S, Buchner R, Kunz W (2005) Percolating microemulsions of nonionic surfactants probed by dielectric spectroscopy. ChemPhysChem 6(6):1051
32. Ponton A, Bose T, Delbos G (1991) Dielectric study of percolation in an oil—continuous microemulsion. J Chem Phys 94:6879
33. Tanaka R, Shiromizu T (2001) Stepwise process forming AOT W/O microemulsion investigated by dielectric measurements. Langmuir 17(26):7995
34. He K, Zhao K, Chai J, Li G (2007) Dielectric analysis of the APG/*n*-butanol/cyclohexane/water nonionic microemulsions. J Colloid Interface Sci 313(2):630
35. Lian Y, Zhao K (2011) Dielectric analysis of micelles and microemulsions formed in a hydrophilic ionic liquid. I. Interaction and percolation. J Phys Chem B 115(39):11368
36. Zhu DM, Schelly Z (1992) Investigation of the microenvironment in Triton X-100 reverse micelles in cyclohexane, using methyl orange as a probe. Langmuir 8(1):48
37. Almgren M, Van Stam J, Swarup S, Löfroth J (1986) Structure and transport in the microemulsion phase of the system Triton X-100-toluene-water. Langmuir 2(4):432
38. Mo C (2002) 1.5-Order differential electroanalysis on Triton X-100 microemulsion. Langmuir 18(10):4047
39. Tabor RF, Eastoe J, Grillo I (2009) Time-resolved small-angle neutron scattering as a lamellar phase evolves into a microemulsion. Soft Matter 5(10):2125
40. Sarkar D, Tikku S, Thapar V, Srinivasa RS, Khilar KC (2011) Formation of zinc oxide nanoparticles of different shapes in water-in-oil microemulsion. Colloids Surf A 381(1):123
41. Rodriguez R, Vargas S, Fernandez-Velasco D (1998) Reverse micelle systems composed of water, Triton X-100, and phospholipids in organic solvents: 1. Phase boundary titrations and dynamic light scattering analysis. J Colloid Interface Sci 197(1):21
42. Schwan HP (1963) Determination of biological impedance. In: Nastuk WL (ed) Physical techniques in biological research, vol 6. Academic Press, NewYork, p 323
43. Cole KS, Cole RH (1941) Dispersion and absorption in dielectrics I. Alternating current characteristics. J Chem Phys 9:341
44. Hanai T (1968) Electrical properties of emulsions. In: Sherman P (ed) Emulsion science. Academic, London, pp 354–477
45. Hanai T, Imakita T, Koizumi N (1982) Analysis of dielectric relaxations of w/o emulsions in the light of theories of interfacial polarization. Colloid Polym Sci 260(11):1029
46. Peyrelasse J, Boned C (1985) Study of the structure of water/aerosol OT/dodecane systems by time domain dielectric spectroscopy. J Chem Phys 89(2):370
47. Bordi F, Cametti C (2001) Occurrence of an intermediate relaxation process in water-in-oil microemulsions below percolation: the electrical modulus formalism. J Colloid Interface Sci 237(2):224
48. Lian Y, Zhao K (2011) Study of micelles and microemulsions formed in a hydrophobic ionic liquid by a dielectric spectroscopy method. I. Interaction and percolation. Soft Matter 7(19):8828
49. Chen Z, Nozaki R (2012) Dielectric spectroscopy study on ionic liquid microemulsion composed of water, TX-100, and BmimPF6. J Chem Phys 136(24):244505